

---

# Interesting properties of GAN samples

---

Anonymous Author(s)

Affiliation

Address

email

## Abstract

1 In this paper we investigate numerical properties of samples produced with ad-  
2 versarial methods, specially Generative Adversarial Networks. We analyze pixel  
3 value statistics of real and generated data and compute distances using the marginal  
4 distribution of perceptually significant features. We provide results on MNIST,  
5 music and speech data and show that GAN generated samples have interesting  
6 signatures that can be used to identify the source of the data and detect adversarial  
7 attacks.

## 1 Introduction

9 Since the groundbreaking Generative Adversarial Networks paper [4] in 2014, most GAN related  
10 publications use a grid of image samples to accompany theoretical and empirical results. Given  
11 this context, the expansion of GAN research to other domains including language models [6] and  
12 music [14] display the need of sample inspection.

13 Unlike Variational Autoencoders (VAEs) and other models [4], most of the evaluation of the output  
14 of Generators trained with the GAN framework is qualitative: authors normally list higher sample  
15 quality as one of the advantages of their method over other methods. Interestingly, little is mentioned  
16 about the numerical properties of GAN samples and how these properties compare to real samples.

17 In the context of Verified Artificial Intelligence[13], it is hard to systematically verify the Generator  
18 and the samples it produces because verification might depend on the existence of perceptually  
19 meaningful features. For example, consider the generation of images of humans: although it is  
20 possible to compare color histograms of real and fake<sup>1</sup> samples, we do not yet have robust algorithms  
21 able to verify if an image follows specifications derived from anatomy.

22 This paper is related to this systematic sample verification and focuses on understanding the numerical  
23 properties of GAN samples. We investigate how the Generator approximates modes in the real  
24 distribution and verify if the generated samples violate specifications derived from the real distribution.  
25 We offer the following contributions in this paper:

- 26 • We show that GAN samples have universal signatures.
- 27 • We show how GAN samples approximate modes of the real distribution.
- 28 • We show significant differences between the marginal distribution of features.
- 29 • We show GAN samples that violate specifications in the real data.

## 30 2 Related work

31 Despite its youth, several publications ([1], [12], [15], [11]) have investigated the use of the GAN  
32 framework for generation of samples and unsupervised feature learning. Following the procedure

---

<sup>1</sup>Generated samples

described in [3] and used in [4], earlier GAN papers evaluated the quality of the Generator by fitting a Gaussian Parzen window<sup>2</sup> to the GAN samples and reporting the log-likelihood of the test set under this distribution. It is known that this method has some drawbacks, including its high variance and bad performance in high dimensional spaces [4].

Unlike other optimization problems, where analysis of the empirical risk is a strong indicator of progress, in GANs the decrease in loss is not always correlated with increase in image quality [2], and thus authors still rely on visual inspection of generated images. Based on visual inspection, authors confirm that they have not observed mode collapse or that their framework is robust to mode collapse if some criteria is met ([2], [6], [8], [11]). In practice, github issues where practitioners report mode collapse or not enough variety abound.

In their brilliant publications, [8], [2] and [6] propose alternative objective functions and algorithms that circumvent problems that are common when using the original GAN objective described in [4]. The problems addressed include instability of learning, mode collapse and meaningful loss curves [12].

These alternatives do not eliminate the need or excitement<sup>3</sup> of visually inspecting GAN samples during training, nor do they provide quantitative information about the generated samples. In the following sections, we will analyze GAN samples and reveal some interesting properties therein. In addition to comparing the marginal distribution of features from the real and fake data, we approach these distributions from the real data as specifications that can be used to validate the output of GAN Samples. We start by enumerating the hypotheses evaluated in this paper.

### 3 Hypotheses

**Hypothesis 1 (H1):** *Generative models can approximate the distribution of real data and hallucinate fake data that has some variety and resembles real data.*

Although this hypothesis is trivial for experiments that have already been conducted, it is the first condition for our experiments. To our knowledge there are no publications where GANs are successful in hallucinating polyphonic music and speech data. During our experiments we prove that these hypotheses hold.

**Hypothesis 2 (H2):** *The real data has useful properties that can be extracted computationally.*

By useful we refer to properties that can be used to describe specifications of the real data. For example, computing the distribution MNIST pixel values might be not useful for assessing drawing quality but it might be useful to evaluate if a random MNIST sample is real or fake.

**Hypothesis 3 (H3):** *The fake data has properties that are hardly noticed with visual inspection of samples.*

Visual inspection of generated samples has become the norm for the evaluation of samples generated using the GAN framework. We investigate if there are properties common to all GAN samples or properties that significantly differ between the real data and the fake data. This hypothesis supports the next hypothesis related to adversarial attacks.

**Hypothesis 4 (H4):** *The difference in properties can be used to identify the source (real or fake)*

The development of generative models foreshadows the imminent rise of adversarial attacks. We investigate if these differences can be used to detect the source of the data (real, GAN or adversarial attack).

With respect to hypotheses 2 and 4, we call the reader’s attention that approximating the distribution over features computed on the real data does not guarantee that the real data is being approximated. Formally speaking: consider  $X \sim Z$ , i.e.  $X$  distributed as  $Z$ , and  $f(X) \sim W$ , where  $f : X \mapsto Y$ . If  $A \sim B$  and  $B$  approximates  $Z$ , then  $f(A) \sim D$  must also approximate  $W$ . However, a distribution that approximates  $W$  is not guaranteed to approximate  $Z$ .

---

<sup>2</sup>Kernel Density Estimation

<sup>3</sup>Despite of authors promising on twitter to never train GANs again.

## 79 4 Methodology

80 In this section we describe our methodology, briefly describing the datasets and features computed,  
81 as well as the model architectures and GAN algorithms used.

### 82 4.1 Datasets

83 In our experiments, we use the MNIST dataset, a MIDI dataset of 389 Bach Chorales downloaded  
84 from the web and a subsample of the NIST 2004 telephone conversational speech dataset with 100  
85 speakers, multiple languages and on average 5 minutes of audio per speaker.

### 86 4.2 Property extraction

87 The properties extracted from the datasets used on this paper can be perceptually meaningful or not.  
88 We claim that both properties can be used to numerically identify the source of the sample. In the  
89 context of this paper, samples are images of size 64 by 64.

#### 90 4.2.1 Spectral Moments

91 The spectral centroid [10] is a feature commonly used in the audio domain, where it represents the  
92 barycenter of the spectrum. This feature can be applied to other domains and we invite the reader  
93 to visualize Figure 1 for examples on MNIST and Mel-Spectrograms [10]. For each column in an  
94 image, we transform the pixel values into row probabilities by normalizing them by the column sum,  
95 after which we take the expected row value, thus obtaining the spectral centroid.

96 Figure 1a shows the spectral centroid computed on sample of MNIST training data.

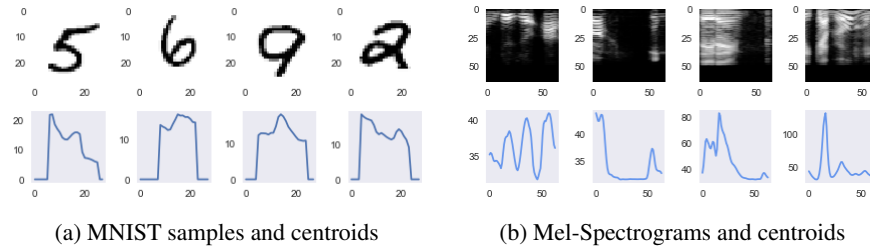


Figure 1: Spectral centroids on digits and Mel-Spectrograms

#### 97 4.2.2 Spectral Slope

98 The spectral slope adapted from [10] is computed by applying linear regression using an overlapping  
99 sliding window of size 7. For each window, we regress the spectral centroids on the column number  
100 *mod* the window size. Figure 2 shows these features computed on MNIST and Mel-Spectrograms.

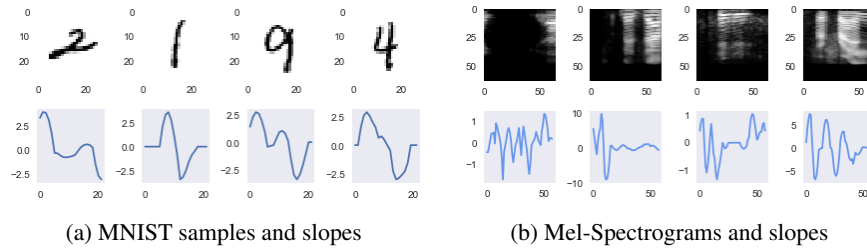


Figure 2: Spectral slopes on digits and Mel-Spectrograms

### 101 4.3 Generative Models

102 We investigate samples produced with the DCGAN architecture using the Least-Squares GAN  
 103 (LSGAN) [8] and the improved Wasserstein GAN (IWGAN) [6]. We also compare adversarial  
 104 MNIST samples produced with the fast gradient sign method (FGSM) [5].

## 105 5 Experiments

### 106 5.1 MNIST

107 We compare the distribution of features computed over the MNIST training set to other datasets,  
 108 including the MNIST test set, samples generated with GANs and adversarial samples computed  
 109 using FGSM. The training data is scaled to  $[0, 1]$  and the random baseline is sampled from a Bernoulli  
 110 distribution with probability equal to the value of pixel intensities in the MNIST training data, 0.13.  
 111 Each GAN model is trained until the loss plateaus and the generated samples look similar to the real  
 112 samples. The datasets compared have 10 thousand samples each.

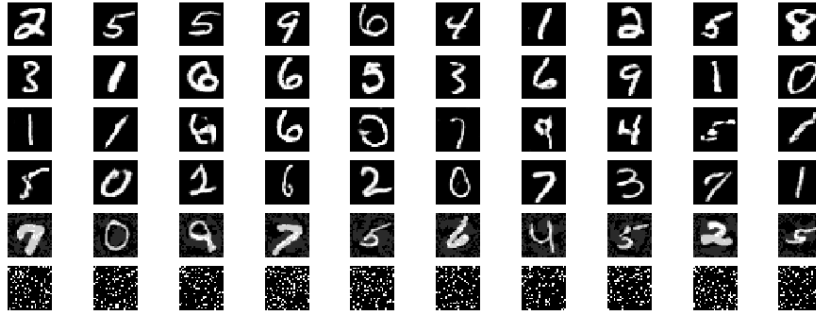


Figure 3: Samples drawn from MNIST train, test, LSGAN, IWGAN, FGSM and bernoulli respectively.

113 Visual inspection of the generated samples in Figure 3 show that IWGAN seems to produce better  
 114 samples than LSGAN. Quantitatively, we use the MNIST training set as a reference and compare the  
 115 distribution of pixel intensities. Table 1 reveals that although samples generated with LSGAN and  
 116 IWGAN look similar to the training set, they are considerably different from the training set given the  
 117 Kolmogorov-Smirnov (KS) Two Sample Test and the Jensen-Shannon Divergence (JSD), specially if  
 118 compared to the same statistics on the MNIST test data.

	KS Two Sample Test		JSD
	Statistic	P-Value	
mnist_train	0.0	1.0	0.0
mnist_test	0.003177	0.0	0.000029
mnist_lsgan	0.808119	0.0	0.013517
mnist_iwgan	0.701573	0.0	0.014662
mnist_adversarial	0.419338	0.0	0.581769
mnist_bernoulli	0.130855	0.0	0.0785009

Table 1: Statistical comparison over the distribution of pixel values for different samples using MNIST training set as reference.

119 These numerical phenomena can be understood by investigating the empirical CDFs in Figure 4. The  
 120 pixel values of the samples generated with the GAN framework are mainly bimodal and asymptotically  
 121 approach the modes of the distribution of pixel values in the real data, 0 and 1. Such behavior will  
 122 be present in any Generator trained using gradient descent and an asymptotically converging non-  
 123 linearity, such as sigmoid and tanh, at the output of the generating function.

124 In addition, Figure 5 shows that the GAN generated samples smoothly approximate the modes of  
 125 the distribution. This smooth approximation is considerably different from the training and test sets.

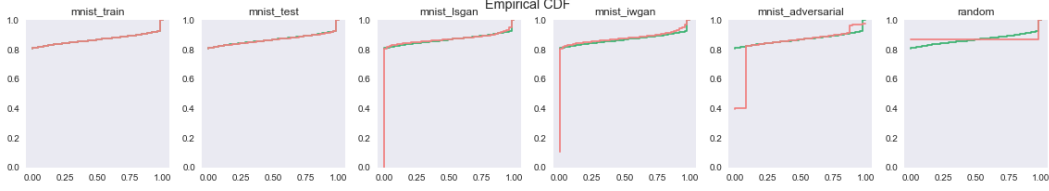


Figure 4: Pixel empirical CDF of training data as reference (green) and other datasets (red)

126 Although these properties are not perceptually meaningful, they can be used to identify the source of  
 127 the data, hence confirming hypotheses 2, 3 and 4.

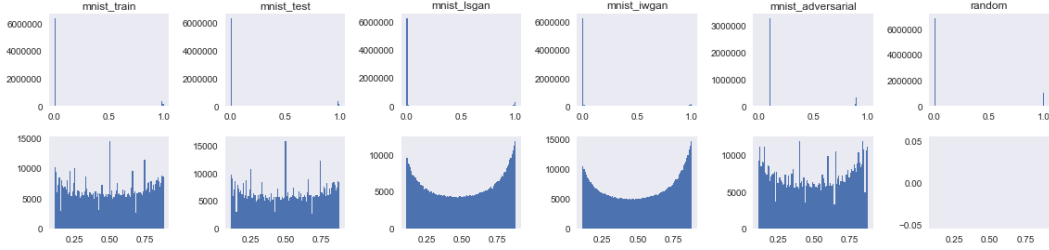


Figure 5: Histogram of pixel intensities for each dataset. First row shows histogram within the [0, 1] interval and 100 bins. Second row shows histograms between the [0.11, and 0.88] interval and 100 bins.

## 128 5.2 Bach Chorales

129 We investigate the properties of Bach chorales generated with the GAN framework and verify if they  
 130 satisfy musical specifications. Bach chorales are polyphonic pieces of music, normally written for 4  
 131 or 5 voices, that follow a set of specifications/rules<sup>4</sup>. For example, a global specification could assert  
 132 that only a set of durations are valid; a local specification could assert that only certain transitions  
 133 between states (notes) are valid depending on the current harmony.

134 For this experiment, we convert the dataset of Bach chorales to piano rolls. The piano roll is a  
 135 representation in which the rows represent note numbers, the columns represent time steps and  
 136 the cell values represent note intensities. We compare the distribution of features computed over  
 137 the training set, test set, GAN generated samples and a random baseline sampled from a Bernoulli  
 138 distribution with probability equal to the normalized mean value of intensities in the training data.  
 139 After scaling, the intensities in the training and test data are strictly bimodal and equal to 0 or 1.  
 140 Figure 6 below shows training, test, IWGAN and Bernoulli samples, thus confirming hypothesis 1.  
 141 Each dataset has roughly 1000 image patches.

142 Figure 7 shows a behavior that is similar to our previous MNIST experiments: the IWGAN asymptotically  
 143 approximates the modes of the distribution of intensity values. In the interest of space, we  
 144 refer the reader to the online appendix<sup>5</sup> for statistics and other relevant information.

145 Following, we investigate if the generated samples violate the specifications of Bach chorales. For  
 146 doing so, we first convert all datasets to boolean by thresholding at 0.5 such that values above the  
 147 threshold are set to 1 or 0 otherwise. We use these piano rolls to compute boolean Chroma [10]  
 148 feature and to compute an empirical Chroma transition matrix, where the positive entries represent  
 149 existing and valid transitions. The transition matrix built on the training data is taken as the reference  
 150 specification, i.e. anything that is not included is a violation of the specification. Table 2 shows  
 151 the number of violations given each dataset. Although Figure 6 shows generated samples that look  
 152 similar to the real data, the IWGAN samples have over 5000 violations, 10 times more than the test  
 153 set! We use these facts to confirm hypotheses 2, 3 and 4.

<sup>4</sup>The specifications define the characteristics of the musical style.

<sup>5</sup>Not provided to preserve anonymity

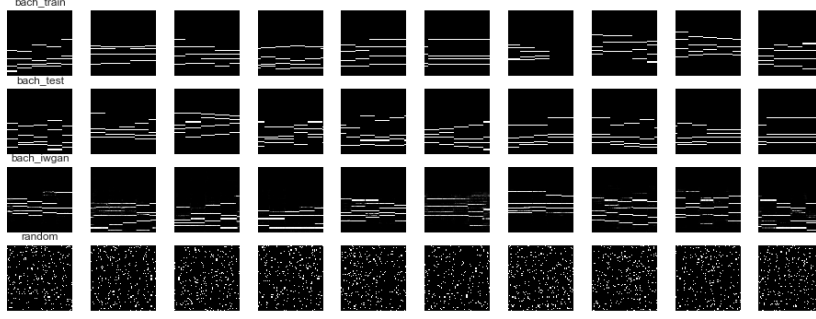


Figure 6: Samples drawn from Bach Chorales train, test, IWGAN, and Bernoulli respectively.

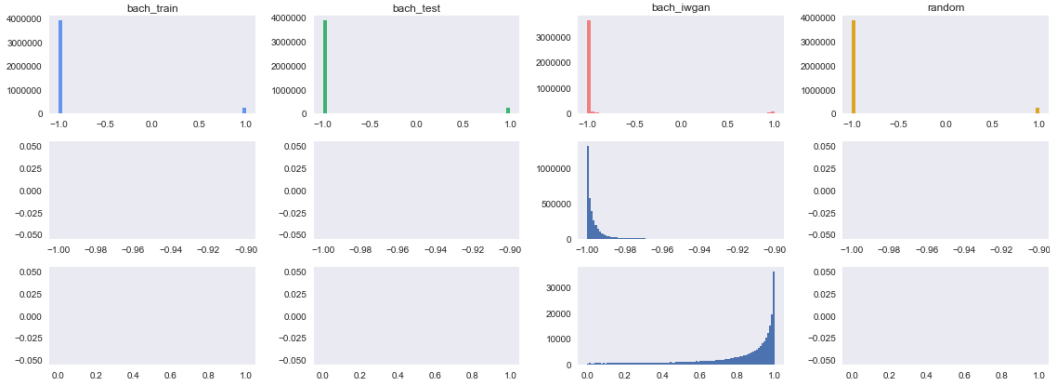
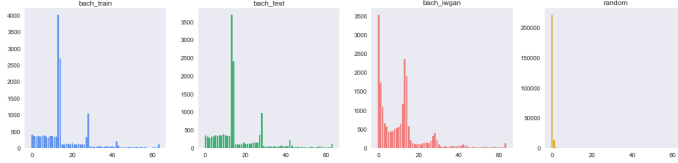


Figure 7

	bach_train	bach_test	bach_iwgan	bach_bernoulli
Number of Violations	0	429	5029	58284

Table 2: Number of specification violations with training data as reference.

In addition to experiments with Chroma features, we computed the distribution of note durations on the boolean piano roll described above. Figure 8a shows the distribution of note durations within each dataset. The train and test data are approximately bimodal and, again, the improved WGAN smoothly approximates the dominating modes of the distribution. Table 8b provides a numerical comparison between datasets.



(a) Histogram of note durations

	KS Two Sample Test		JSD
	Statistic	P-Value	
train	0.0	1.0	0.0
test	0.09375	0.929	0.002
iwgan	0.21875	0.080	0.084
bernoulli	0.93750	0.0	0.604

(b) Test statistics

### 5.3 Speech

Within the speech domain, we investigate dynamic compressed Mel-Spectrogram samples produced with GANs trained on a subset of the NIST 2004 dataset, with 100 speakers. We divide the NIST 2004 dataset into training and test set, generate samples with the GAN framework and use a random baseline sampled from a Exponential distribution with parameters chosen using heuristics. The generated samples can be seen in Figure 9, thus confirming hypothesis 1. We obtain the Mel-Spectrogram by projecting a spectrogram onto a mel scale, which we do with the python library

librosa [9]. More specifically, we project the spectrogram onto 64 mel bands, with window size equal to 1024 samples and hop size equal to 160 samples, i.e. frames of 100ms long. Dynamic range compression is computed as described in [7], with  $\log(1 + C * M)$ , where  $C$  is the compression constant scalar set to 1000 and  $M$  is the matrix representing the Mel-Spectrogram. Each dataset has approximately 1000 image patches and the GAN models are trained using DCGAN with the improved Wasserstein GAN algorithm.

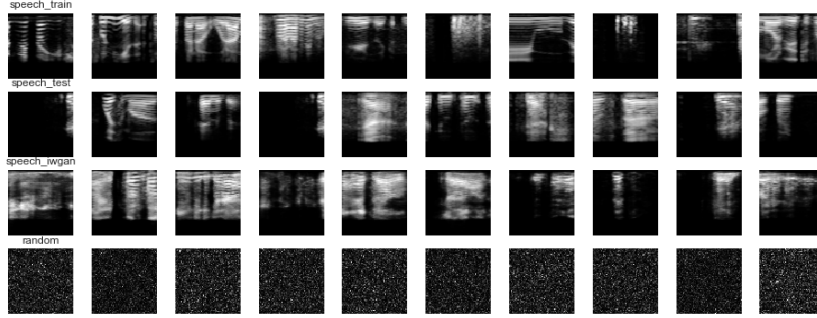
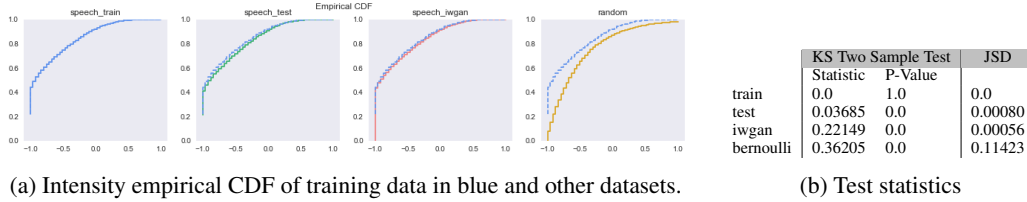


Figure 9: Samples drawn from Mel-Spectrogram Speech train, test, IWGAN, and exponential respectively.

In Figure 10a we show the empirical CDFs of intensity values. Unlike our previous experiments where intensity (Bach Chorales) or pixel value (MNIST) was linear, in this experiment intensities are compressed using the log function. This considerably reduces the distance between the empirical CDFs of the training data and GAN samples, specially around the saturating points of the tanh non-linearity,  $-1$  and  $1$  in this case. In Table 10b we show numerical analysis of the differences and confirm hypotheses 2 and 3.



(a) Intensity empirical CDF of training data in blue and other datasets.

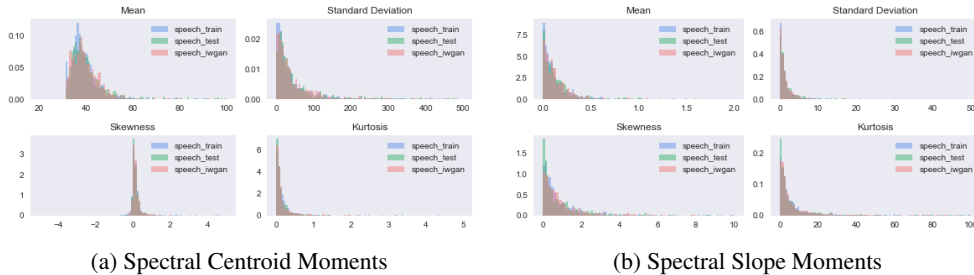
(b) Test statistics

Figure 10: Empirical CDF and statistical tests of speech intensity

177

Figure 11 shows the distribution of statistical moments computed on spectral centroids and slope. The distributions from different sources considerably overlap, indicating that the generator has efficiently approximated the real distribution of these features.

180



(a) Spectral Centroid Moments

(b) Spectral Slope Moments

Figure 11: Moments of spectral centroid (left) and slope(right)

Figure 12 shows statistics used to compare the reference (training data) and other datasets. The difference between KS-Statistics and JSD of the test data and generated samples are negligible. Interestingly, the p-values of the spectral slope of the improved WGAN are considerably higher

than the test data. For these reasons and although Table 10b shows a significant difference between the KS-Statistic of test data and generated data with respect to the training data, we refrain from confirming hypothesis 4. An adversary can easily manipulate the generated data to considerably decrease this difference and still keep the high similarity in features harder to simulate such as moments of spectral centroid or slope.

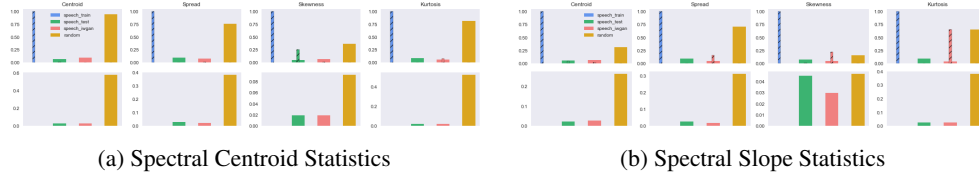


Figure 12: Statistics of spectral centroid (left) and slope(right)

## 6 Conclusions

In this paper we investigated numerical properties of samples produced with adversarial methods, specially Generative Adversarial Networks. We showed that GAN samples have universal signatures that are dependent on the choice of non-linearity on the last layer of the generator. In addition, we showed that adversarial examples produced with the FSGM have properties that can be used to identify an adversarial attack. Following, we showed that GAN samples smoothly approximate the dominating modes of the distribution and that this information can be used to identify the source of the data. Last, we showed that samples generated with GANs violate specifications and do not provide guarantees on satisfaction of simple specifications. With this we hope to call attention to the necessity of the development of verified AI and better understanding of GAN generated samples.

## Acknowledgments

## References

- [1] Martin Arjovsky and Léon Bottou. Towards principled methods for training generative adversarial networks. In *NIPS 2016 Workshop on Adversarial Training. In review for ICLR*, volume 2016, 2017.
- [2] Martin Arjovsky, Soumith Chintala, and Léon Bottou. Wasserstein gan. *arXiv preprint arXiv:1701.07875*, 2017.
- [3] Olivier Breuleux, Yoshua Bengio, and Pascal Vincent. Quickly generating representative samples from an rbm-derived process. *Neural Computation*, 23(8):2058–2073, 2011.
- [4] Ian Goodfellow, Jean Pouget-Abadie, Mehdi Mirza, Bing Xu, David Warde-Farley, Sherjil Ozair, Aaron Courville, and Yoshua Bengio. Generative adversarial nets. In *Advances in neural information processing systems*, pages 2672–2680, 2014.
- [5] Ian J Goodfellow, Jonathon Shlens, and Christian Szegedy. Explaining and harnessing adversarial examples. *arXiv preprint arXiv:1412.6572*, 2014.
- [6] Ishaan Gulrajani, Faruk Ahmed, Martin Arjovsky, Vincent Dumoulin, and Aaron Courville. Improved training of wasserstein gans. *arXiv preprint arXiv:1704.00028*, 2017.
- [7] Yanick Lukic, Carlo Vogt, Oliver Dürr, and Thilo Stadelmann. Speaker identification and clustering using convolutional neural networks. In *Machine Learning for Signal Processing (MLSP), 2016 IEEE 26th International Workshop on*, pages 1–6. IEEE, 2016.
- [8] Xudong Mao, Qing Li, Haoran Xie, Raymond YK Lau, Zhen Wang, and Stephen Paul Smolley. Least squares generative adversarial networks. *arXiv preprint ArXiv:1611.04076*, 2016.
- [9] Brian McFee, Colin Raffel, Dawen Liang, Daniel PW Ellis, Matt McVicar, Eric Battenberg, and Oriol Nieto. librosa: Audio and music signal analysis in python. In *Proceedings of the 14th python in science conference*, 2015.



- 223 [10] Geoffroy Peeters. A large set of audio features for sound description (similarity and classifica-  
224 tion) in the cuidado project. Technical report, 2004.
- 225 [11] Alec Radford, Luke Metz, and Soumith Chintala. Unsupervised representation learning with  
226 deep convolutional generative adversarial networks. *arXiv preprint arXiv:1511.06434*, 2015.
- 227 [12] Tim Salimans, Ian J. Goodfellow, Wojciech Zaremba, Vicki Cheung, Alec Radford, and Xi Chen.  
228 Improved techniques for training gans. *CoRR*, abs/1606.03498, 2016.
- 229 [13] Sanjit A. Seshia and Dorsa Sadigh. Towards verified artificial intelligence. *CoRR*,  
230 abs/1606.08514, 2016.
- 231 [14] Li-Chia Yang, Szu-Yu Chou, and Yi-Hsuan Yang. Midinet: A convolutional generative ad-  
232 versarial network for symbolic-domain music generation using 1d and 2d conditions. *CoRR*,  
233 abs/1703.10847, 2017.
- 234 [15] Junbo Zhao, Michael Mathieu, and Yann LeCun. Energy-based generative adversarial network.  
235 *arXiv preprint arXiv:1609.03126*, 2016.